Acute particulate matter (PM10) exposure selectively triggers behavioral alterations in the presymptomatic Experimental Autoimmune Encephalomyelitis (EAE) mouse model of Multiple Sclerosis

Acute particulate matter (PM_{10}) exposure selectively triggers behavioral alterations in the presymptomatic Experimental Autoimmune Encephalomyelitis (EAE) mouse model of Multiple Sclerosis

Martino Bonato*[1], Francesca Montarolo*[2], Roberta Parolisi[3], Silvia De Francia[4], Claudio Pandino[5], Niccolò Di Cintio[6], Antonio Bertolotto[7], Annalisa Buffo[8], Enrica Boda[9]

[1] Neuroscience Institute Cavalieri Ottolenghi (NICO), Department of Neuroscience Rita Levi-Montalcini, University of Turin, Regione Gonzole, 10 – 10043 Orbassano (Turin), Italy. martino.bonato@unito.it

[2] Neuroscience Institute Cavalieri Ottolenghi (NICO), Department of Neuroscience Rita Levi-Montalcini, University of Turin, Regione Gonzole, 10 – 10043 Orbassano (Turin), Italy. francesca.montarolo@unito.it

[3] Neuroscience Institute Cavalieri Ottolenghi (NICO), Department of Neuroscience Rita Levi-Montalcini, University of Turin, Regione Gonzole, 10 – 10043 Orbassano (Turin), Italy. roberta.parolisi@unito.it

[4] Department of Clinical and Biological Sciences, University of Turin, Regione Gonzole, 10 – 10043 Orbassano (Turin), Italy. silvia.defrancia@unito.it

[5] Neuroscience Institute Cavalieri Ottolenghi (NICO), Department of Neuroscience Rita Levi-Montalcini, University of Turin, Regione Gonzole, 10 – 10043 Orbassano (Turin), Italy. claudio.pandino@edu.unito.it

[6] Neuroscience Institute Cavalieri Ottolenghi (NICO), Department of Neuroscience Rita Levi-Montalcini, University of Turin, Regione Gonzole, 10 – 10043 Orbassano (Turin), Italy. niccolo.dicintio@unito.it

[7] Neuroscience Institute Cavalieri Ottolenghi (NICO), Regione Gonzole, 10 – 10043 Orbassano (Turin), Italy. Koelliker Hospital, Corso Galileo Ferraris, 247-255 – 10134 Turin, Italy. antonio.bertolotto@gmail.com

[8] Neuroscience Institute Cavalieri Ottolenghi (NICO), Department of Neuroscience Rita Levi-Montalcini, University of Turin, Regione Gonzole, 10 – 10043 Orbassano (Turin), Italy. annalisa.buffo@unito.it

[9] Neuroscience Institute Cavalieri Ottolenghi (NICO), Department of Neuroscience Rita Levi-Montalcini, University of Turin, Regione Gonzole, 10 – 10043 Orbassano (Turin), Italy. enrica.boda@unito.it

* equal contribution

Corresponding author:

Enrica Boda

ORCID ID: 0000-0002-1006-2577

Department of Neuroscience Rita Levi Montalcini, Neuroscience Institute Cavalieri Ottolenghi (NICO), University of Turin, Regione Gonzole, 10 – 10043 Orbassano (Turin), Italy

enrica.boda@unito.it

Data availability statement

All data are available in the main text or in the Source data file enclosed as supplementary material.

Conflict of interest disclosure

The authors declare no conflict of interest. The funding sponsors had no role in the interpretation of data or in the writing of the manuscript.

Funding statement

Our work was supported by FISM - Fondazione Italiana Sclerosi Multipla (Italy) (ID:2019/PR-Multi/003) and by Cassa di Risparmio di Torino (CRT) Foundation grant (ID: 2021.0657) to EB. MB was supported by a PON R&I 2014-2020 PhD Fellowship “Dottorati di ricerca su tematiche green e dell’innovazione”, financed by Ministero dell’Istruzione, dell’Università e della Ricerca—MIUR (Italy) in the frame of FSE– REACT EU. This study was also supported by Ministero dell’Istruzione, dell’Università e della Ricerca—MIUR (Italy) project “Dipartimenti di Eccellenza 2018–2022” and “Dipartimenti di Eccellenza 2013–2027” to Dept. of Neuroscience “Rita Levi Montalcini” of the University of Turin.

Ethics approval statement

The study involves experimental animals and was designed according to the guidelines of the European Communities Council (2010/63/EU) and the Italian Law for Care and Use of Experimental Animals (DL26/2014). It was also approved by the Italian Ministry of Health and the Bioethical Committee of the University of Turin. The study was conducted according to the ARRIVE guidelines.

Running title: PM_{10} elicits behavioral alterations in EAE mice

Keywords: air pollution, particulate matter, experimental autoimmune encephalomyelitis, Multiple Sclerosis, behavior

Abstract

Multiple Sclerosis (MS) is a chronic disease of the Central Nervous System, where neuroinflammation and autoimmune response against myelin lead to functional impairments and psychiatric symptoms. Exposure to air pollution – and, in particular, to peaks of particulate matter (PM) – has been associated with an increase of hospital admissions for MS onset and relapses and exacerbated neuroinflammation in MS patients. Here, in the MOG_{35-55}-induced experimental autoimmune encephalomyelitis (EAE) mouse model of MS, we tested the hypothesis that exposure to PM_{10} might influence the disease course and severity in individuals with a predisposing background. Short-term PM_{10} exposures - occurring either before immunization or during the pre-symptomatic phase - did not modify disease manifestation in EAE mice, as assessed by clinical and neuropathological analyses. Yet, presymptomatic EAE – but not healthy - mice selectively showed increased disinhibited, risk-taking and novelty-seeking behaviors early after being exposed to PM_{10}. These data show a selective vulnerability of immunologically primed mice toward the effects of PM_{10}, occurring before the emergence of overt motor impairment and presenting as specific behavioral alterations.

Introduction

The pathogenesis of autoimmune diseases – such as Multiple Sclerosis (MS) - is thought to have a strong genetic background component, but a substantial impact of environmental risk factors – including exposure to air pollution, tobacco smoking, infections or drugs – has been also recognized in either the development or the exacerbation of these conditions (Sellner et al., 2011; Gawda et al., 2017). MS is a chronic autoimmune disease of the Central Nervous System (CNS) - characterized by neuroinflammation, multifocal demyelination, and eventually neurodegeneration - leading to functional impairments and - in most cases - psychiatric symptoms (Woo et al., 2024; Benedict et al., 2020; Sparaco et al., 2021). Studies have linked exposure to air pollution – and, in particular, short-term increases in airborne particulate matter (PM) - with an increased incidence of hospital admissions for MS onset and relapses (Angelici et al., 2016; Roux et al., 2017, Heydarpour et al., 2014; Oikonen et al., 2003; Gregory et al., 2008; Noorimotlagh et al., 2021). This suggests that even acute exposures to high levels of PM might accelerate the onset of MS in individuals with a predisposing background, or trigger the worsening of the disease in MS patients (Bergamaschi et al., 2021).

Despite recent improvements in air quality, air pollution is still the largest environmental health risk in Europe, where more than 80% of the urban population is exposed to unsafe concentrations of PM, according to the World Health Organization (WHO) Air Quality Guidelines (Europe's air quality status 2024 released by the European Environment Agency ; https://www.eea.europa.eu//publications/europes-air-quality-status-2024). PM is a mixture of particles - typically including inorganic compounds, aromatic hydrocarbons (e.g. benzene), metals, and microbial components (e.g. lipopolysaccharide (Becker et al., 2002)) - released from the combustion of fossil fuels, gasoline, diesel, coal, or wood, as well as from natural events like volcanic eruptions, soil and rocks erosion (Sierra-Vargas et al., 2012). PM particles are categorized by their size, with coarse particles (i.e. PM_{10}) and fine particles (i.e. $PM_{2.5}$) having aerodynamic diameters smaller than 10 and 2.5 μm, respectively. Thanks to their size, PM particles can penetrate the respiratory tract up to the alveoli. Here, PM initiates a local oxidative-inflammatory reaction that eventually extends and disrupts the homeostasis of various distant organs and systems, including the CNS (Peeples, 2020). Consistently, even in healthy subjects, residency in cities with high air pollution including PM, is associated with neuroinflammation, white matter injury, disruption of the blood brain barrier (BBB) integrity and altered brain innate immune activity (Calderón-Garcidueñas et al., 2008; Babadjouni et al., 2017). Such a response appears to be amplified in MS patients, where PM exposure correlates with brain inflammatory exacerbation as detected by MRI with gadolinium (Bergamaschi et al., 2017). Also, of relevance for MS, higher concentration of antibodies directed against myelin proteins have been found in the serum and in the cerebrospinal fluid (CSF) of people resident in metropolitan city areas with high levels of airborne PM (Calderón-Garcidueñas et al.,

2015). Besides this correlative evidence in humans, controlled studies in experimental animal models have revealed that PM exposure causes neurovascular inflammation, BBB functional deficits (Nejad et al., 2014), microglia activation and demyelination (Woodward et al., 2017; Han et al., 2022). We also recently found that an acute exposure to PM targets the endogenous regenerative capability of the CNS tissue by hampering remyelination and promoting astroglia and microglia reactivity in the mouse (Parolisi et al., 2021).

Thus, there is now a strong rationale to hypothesize that even a short-term exposure to PM can interact or even synergize with the individual's immune background and contribute to MS pathogenesis or exacerbation. To address this issue, we investigated whether an acute exposure to PM_{10} - occurring either before the immunization or during the pre-symptomatic phase - affects the disease course and the behavioral phenotype of an animal model of MS, i.e. the chronic MOG_{35-55}-induced experimental autoimmune encephalomyelitis (EAE). While acute PM_{10} exposures did not significantly accelerate the emergence of motor deficits, nor modified the disease course in EAE mice, presymptomatic EAE – but not healthy - mice selectively showed increased disinhibited, risk-taking and novelty-seeking behaviors after being exposed to PM_{10}. To assess the biological substrate of the selective response of EAE mice to PM_{10}, we investigated possible alterations of the dopaminergic neurotransmission, which were formerly associated with a behavioral phenotype reminiscent of that observed in PM_{10}-exposed EAE mice (Pogorelov et al., 2005; Kalueff et al., 2016). Yet, no change in dopamine availability or in the expression of genes coding for dopamine receptors, transporters and synthetic/degrading enzymes have been detected in the mouse brain as associated with PM_{10} exposure. Overall, data show a selective vulnerability of immunologically primed mice toward the effects of PM_{10}, occurring before the emergence of overt motor impairment and presenting as specific behavioral alterations.

Materials and Methods

Animals and experimental design

Mice were housed in the vivarium under standard conditions (12-hr light/12-hr dark cycle at 21°C) with food and water ad libitum. The project was designed according to the guidelines of the NIH, the European Communities Council (2010/63/EU) and the Italian Law for Care and Use of Experimental Animals (DL26/2014). It was also approved by the Italian Ministry of Health (authorization 510/ 2020-PR to EB) and the Bioethical Committee of the University of Turin. The study was conducted according to the ARRIVE guidelines.

Chronic EAE induction and evaluation of the clinical score

To induce chronic EAE, 8 week-old female C57BL/6J mice (Charles River, Calco, Italy) were immunized by 2 subcutaneous injections of 200 µg myelin oligodendrocyte glycoprotein 35-55 peptide (MOG35–55; Espikem, Florence, Italy) in incomplete Freund's adjuvant (IFA; Sigma-Aldrich, Milan, Italy) containing 8 mg/ml Mycobacterium tuberculosis (strain H37Ra; Difco Laboratories Inc., Franklin Lakes, NJ, USA), followed by 2 intravenous injections of 500 ng of Pertussis toxin (Duotech, Milan, Italy) on the immunization day and 48 h later (Montarolo et al., 2015). Body weight and clinical score of each individual mouse were recorded daily by an operator blind to the mouse treatment (i.e. PM *vs.* saline, see below) for 21 days. The clinical score was designed to evaluate the differences in the onset and course of the pathology following the severity of motor defect symptoms, and the score was set as follows: 0=healthy; 1=limp tail; 2=ataxia and/or paresis of hindlimbs; 3=paralysis of hindlimbs and/or paresis of forelimbs; 4=tetraplegia; 5=moribund or dead. Median clinical score was calculated for each group per day to analyze the disease course of the EAE. Cumulative and maximum score, as well as the percentage of disease-free (score=0) mice were also calculated.

PM_{10} administration

We exposed healthy (Ctrl) and EAE mice to a commercially available PM_{10} (NIST Standard Reference Material 1648a; Sigma-Aldrich), which is a chemically standardized compound widely used in toxicological studies (Akhtar et al., 2013; Kewcharoenwong et al., 2023; Gałuszka-Bulaga et al., 2023). Stock suspensions of NIST SRM 1648 PM were prepared in sterile ultrapure water and aliquots were thoroughly mixed under sonication for 1 h prior to each experiment. Mice were randomly divided into control (saline) and treatment (PM) groups. The treatment group was treated by intratracheal instillations (Intubation stand, Kent Scientific Corporation) of a PM_{10} suspension (10 µg in 50 µl of saline), and the control group was treated with saline (50 µl), as in our previous study (Parolisi et al., 2021). We opted for the intratracheal administration of PM to assure low variability of absorption and to exclude a direct nose-to-CNS transit of PM via the olfactory mucosa.

PM_{10} dose was calculated considering the daily respiratory volume of mice (0.04 m^3) and the daily peaks of PM_{10} concentration in East Europe polluted areas (>250 µg/m^3; Zibert et al., 2016). Therefore, in order to use a PM_{10} dose relevant for human exposure, the dose used in this study was set as 10 µg (0.04 m^3/day × 250 µg/m^3). Two different protocols of acute exposure were adopted: a pre-immunization protocol, where PM_{10} was administered 3 days and 1 day before EAE immunization; and a post-immunization protocol, where PM_{10} was administered 4 and 6 days after EAE immunization. Both protocols assured administration of PM_{10} during the presymptomatic phase of the EAE model, where debilitating symptoms are yet to be displayed by the animals.

Behavioral Tests

Tests were performed 6 days after EAE immunization (i.e.in the presymptomatic phase), 6 hours after the second exposure to PM_{10} or saline to both EAE and Ctrl mice. Animals were habituated to the testing room in single transparent cages (36 x 21 x 14 cm height) for at least 1 hour before the test. Analysis was performed by an operator blind to the treatment of the animals, and mouse performance was video recorded with the operator outside the testing room.

Open field (OF) test

Locomotor activity was investigated by means of the OF test, under dim white light conditions (2 lux). Each animal was placed in the corner of the arena (50 × 50 cm) and let explore the arena for 1 h under videorecording. Total distance and distance traveled in the center (25 × 25 cm) of the arena were analyzed using Ethovision XT video track system (Noldus Information Technology, Wageningen, The Netherlands, RRID:SCR_000441).

Analysis of the stereotypic behaviors

Video recordings obtained during the OF test were also analyzed to highlight patterns of stereotypic behaviors, such as grooming (i.e. cleaning of the fur of the head/snout with forepaws, adjusting of posture) and rearing (i.e. extension of the mouse forelimbs when standing on the hindlimbs). Using the open-source Behavioral Observation Research Interactive Software (BORIS, www.boris.unito.it, RRID:SCR_025700) for behavioral quantification, each stereotypic behavior was measured for total events (i.e. number of time the animal performed the action) and total time (i.e. seconds or minutes spent in total by the animal performing a single behavior).

Elevated Plus Maze (EPM) test

The EPM test was used to evaluate anxious behaviors. The apparatus used for the test is a plus-cross shaped platform made in gray forex and raised 60 cm above floor level. The platform comprises two open arms (30 x 5 x 0.20 cm) and two closed arms (30 x 5 x 15 cm walls) originating from a central square platform (5 x 5 cm). At the beginning of each trial, each mouse was gently placed on

the center of the square platform and allowed to explore the maze for 5 minutes under videorecording. The number of entries and the cumulative time spent in either open or closed arms was measured with the Ethovision XT software (RRID:SCR_000441). Animals were considered to have entered an arm of the maze when all four paws left the center of the square.

Novel Object Location (NOL) Test

The test comprised three distinct phases: a first phase of habituation with an empty enclosed arena (33 x 33 cm); a second phase, where two identical objects have been placed into the arena (each object was situated near the corners of one side of the arena); and a third phase, where one of the two objects has been moved to the opposite side of the arena. Inter-trial interval was 10 minutes. During each phase, the animal could freely explore the arena for 10 minutes under videorecording. Mouse movement and interaction with the objects have been tracked using the Ethovision XT software (RRID:SCR_000441).

Tail suspension test

Mice were suspended by the tail into an apparatus (20 x 40 x 60 cm) with white walls and an open side to be video recorded. The animals were attached to the apparatus by adhesive tape wrapped at 1 cm from the tip of the tail. A solid white divisor allowed for simultaneous testing of two mice. Each trial lasted for 6 minutes, and immobility time of each mouse was manually measured (immobility was determined as absence of struggles/movement for >1s). Percentage of time of immobility and latency to first immobility were used to assess depressive symptoms.

Histological Analyses

At 21 days post-immunization (dpi), animals were deeply anesthetized (ketamine-xylazine 90 mg/kg and 9 mg/kg, respectively) and transcardially perfused with 4% paraformaldehyde (PFA) in 0.1 M phosphate buffer (PB). Brains and spinal cords were postfixed overnight, cryoprotected, cut in 30 µm thick sections, and processed according to standard immunohistological procedures (Boda et al., 2022). Sections of the lumbar enlargement of the spinal cord were collected in PBS and then stained to detect the expression of different antigens: MOG (myelin oligodendrocyte glycoprotein; 1:1000, Proteintech Cat# 12690-1-AP, RRID:AB_2145527) to visualize myelination; IBA1 (ionized calcium-binding adapter molecule 1; 1:1000, FUJIFILM Wako Pure Chemical Corporation Cat# 019-19741, RRID:AB_839504), as a microglia marker; GFAP (glial fibrillary acid protein; 1:1000, Agilent Cat# GA524, RRID:AB_2811722) as a marker of astrocytes. Incubation with primary antibodies was made overnight at 4 °C in PBS with 1% Triton-X 100. The sections were then exposed for 2 h at room temperature (RT) to secondary Cy3 (1:500, Jackson ImmunoResearch Labs Cat# 711-165-152, RRID:AB_2307443) or Alexa Fluor 488 (1:500, Jackson ImmunoResearch Labs Cat# 711-545-152, RRID:AB_2313584)/Alexa Fluor 647 (1:500, Jackson ImmunoResearch Labs Cat# 711-605-

152, RRID:AB_2492288) -conjugated antibodies. After processing, sections were mounted on microscope slides with Tris-glycerol supplemented with 10% Mowiol (Calbiochem, LaJolla, CA).

Image processing and data analysis

Histological specimens were examined with a Zeiss Axioscan Z.1 Slide Scanner, which allowed precise tile-scanning of whole-section images. Images were acquired at 20×. Quantitative evaluations were performed on images with ImageJ (Research Service Branch, National Institutes of Health, Bethesda, MD; available at http://rsb.info.nih.gov/ij/; RRID:SCR_003070). To analyze the expression level of MOG, IBA1 and GFAP in the lesion area, the positive fractioned area (i.e. the percentage of positive pixels throughout the entire lesioned area) was quantified. Six animals/group and 10-15 sections per animal were analyzed for each experimental condition. Adobe Photoshop 6.0 (Adobe Systems, San Jose, CA, RRID:SCR_014199) was used to assemble the final plates.

Quantification of dopamine in the mouse brain tissue

Dopamine (DA) concentration was measured in the brain tissue of Ctrl and EAE mice sacrificed 6 hours after exposure to saline or PM_{10}, as reported in (Montarolo et al., 2022). Brains were stored at −80°C until use. DA hydrochloride (analytical standard grade), formic acid (HPLC grade), and ammonium formate (HPLC grade) were purchased from Sigma-Aldrich Corporation (Milan, Italy). Acetonitrile (HPLC grade) was purchased from VWR (Milan, Italy). HPLC-grade water was produced by a Milli-DI system coupled with a Synergy 185 system by Millipore (Milan, Italy). Previously weighted brain samples were immersed in liquid nitrogen, sonicated for 1 min, reconstituted in 1 ml of water, and sonicated for another min. The calibration curve of DA was established in the concentration range of 0.01–5.00 µg/ml. One hundred microliter brain samples were extracted by protein precipitation using 300 µl of freeze solution of formic acid 0.5%v/v in acetonitrile. Each sample was mixed for at least 15″ and then stored in freezer at −20°C for 15′ and later centrifuged at 4000 rpm for 10 min. 250 µl of supernatant were transferred to an injection vial. Chromatographic separation was performed at 35°C, using a column oven, on a RP column (Atlantis T3 4.6 × 50 mm, 5 µm, Waters, USA. The flow rate was set at 1 ml/min. DA brain concentration was reported in µg/mg of tissue weight. For DA quantification, the limit of detectable (LOD) and limit of quantification (LOQ) in the chromatographic method for determining DA were optimized with mixing homogenous samples.

Quantitative RT-PCR

RNA extraction, reverse transcription and quantitative Real Time RT-PCR was performed as described in (Boda et al., 2022 and Boda et al., 2011), either with predeveloped Taqman assays (Applied Biosystems, Thermofisher, Waltham, USA) or by combining the RealTime Ready Universal Probe Library (UPL, Roche Diagnostics, Monza, Italy) with the primers listed in Supplementary Table

2. Real Time data were collected on the Applied Biosystems StepOnePlus Real-Time PCR System with StepOne™ Software (RRID:SCR_014281). Data analysis was performed with Microsoft Excel (Microsoft Office 365, RRID:SCR_016137). A relative quantification approach was used, according to the 2-ddCT method. β-actin was used to normalize expression levels.

Statistical Analyses

Statistical analyses were carried out with GraphPad Prism 9 (GraphPad software, Inc, RRID:SCR_002798). The Shapiro-Wilk test was first applied to test for a normal distribution of the data. When normally distributed, unpaired Student's t-test (to compare two groups) and Two-ways ANOVA test (for multiple group comparisons) followed by Bonferroni's post-hoc analysis, were used. Alternatively, when data were not normally distributed, Mann–Whitney U-test (to compare two groups) was used. The Kaplan-Meier test was used to compare percentages of disease-free mice over time. In all instances, $P < 0.05$ was considered as statistically significant. Graphs represent individual data and mean ± standard error (SE). Statistical differences were indicated with * $P < 0.05$, ** $P < 0.01$, *** $P < 0.001$, **** $P < 0.0001$. The list of the applied tests and number of animals in each case are included in Suppl. Table 1.

Results

Acute exposure to PM_{10} does not modify EAE disease course

In order to validate PM exposure as a contributing factor for disease onset/worsening in an animal model of MS, we have combined the induction of chronic EAE in mice and PM_{10} exposure. Specifically, to assess whether PM operates either by facilitating the induction of autoimmunity (thereby contributing to the initiation of the pathology) or by exacerbating an already established pathological setting (thereby operating as a secondary stressor), mice were acutely exposed to PM_{10} (or saline, as a control) either before the immunization (Fig.1**a**) or during the pre-symptomatic phase (Fig.2**a**), respectively. Daily assessment of the mouse clinical score and body weight, performed for 21 days after EAE immunization, showed that acute PM_{10} exposures did not accelerate the emergence of motor deficits, nor modified the disease course in EAE mice (Fig. 1**b**,**c**; Fig. 2**b**,**c**). The percentage of disease-free mice over time as well as maximum and cumulative EAE scores were also not significantly affected by pre- and post-immunization PM_{10} exposures (Fig. 1**d**-**f**; Fig. 2**d**-**f**). Consistently, post-immunization exposure to PM_{10} did not affect the neuropathology of the lumbar enlargement of the spinal cord in EAE mice, as assessed at 21 dpi. Specifically, the extent of demyelination (as assessed by the MOG-negative area; Fig. 3**a**-**c**), the abundance and hypertrophy of astrocytes (i.e. the GFAP-positive area; Fig. 3**d**-**f**) and microglia (i.e. the IBA1-positive area; Fig. 3**g**-**i**) did not differ in PM_{10}- *vs*. saline-exposed EAE mice.

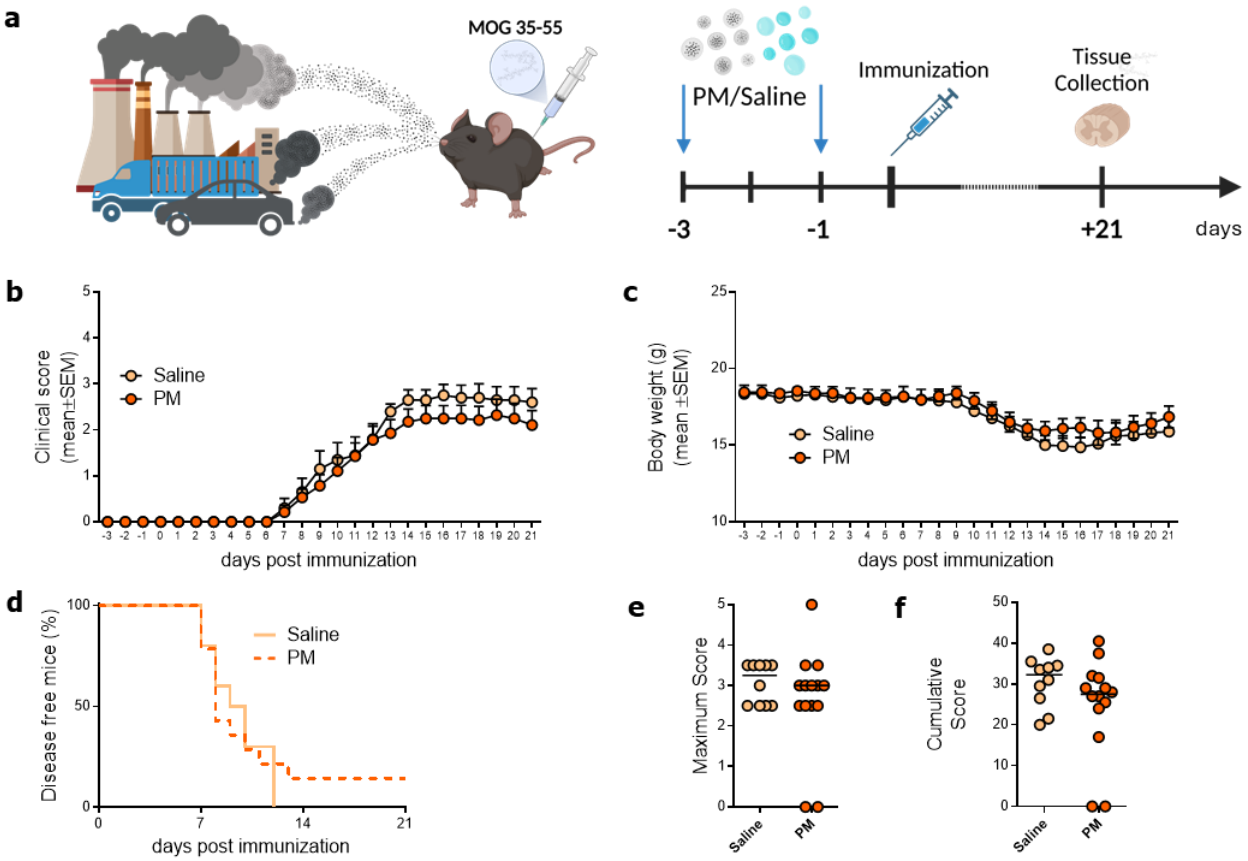

Figure 1 - Pre-immunization exposure to PM_{10} does not alter EAE pathological course

(**a**) Schematic representation of the experimental design (graphics created with BioRender.com). (**b**) Mean clinical score of saline vs. PM_{10}-exposed EAE mice. (**c**) Mean body weight of saline *vs.* PM_{10}-exposed EAE mice during the pathological course. (**d**) Percentage of disease-free mice after EAE immunization. (**e**) Maximum clinical score reached by EAE mice during the pathological course. (**f**) Cumulative score obtained by saline or PM_{10}-exposed EAE mice in 21 days of assessment. Each dot in (**e,f**) represents an individual mouse. Source data are provided as a Source Data file (supplementary material).

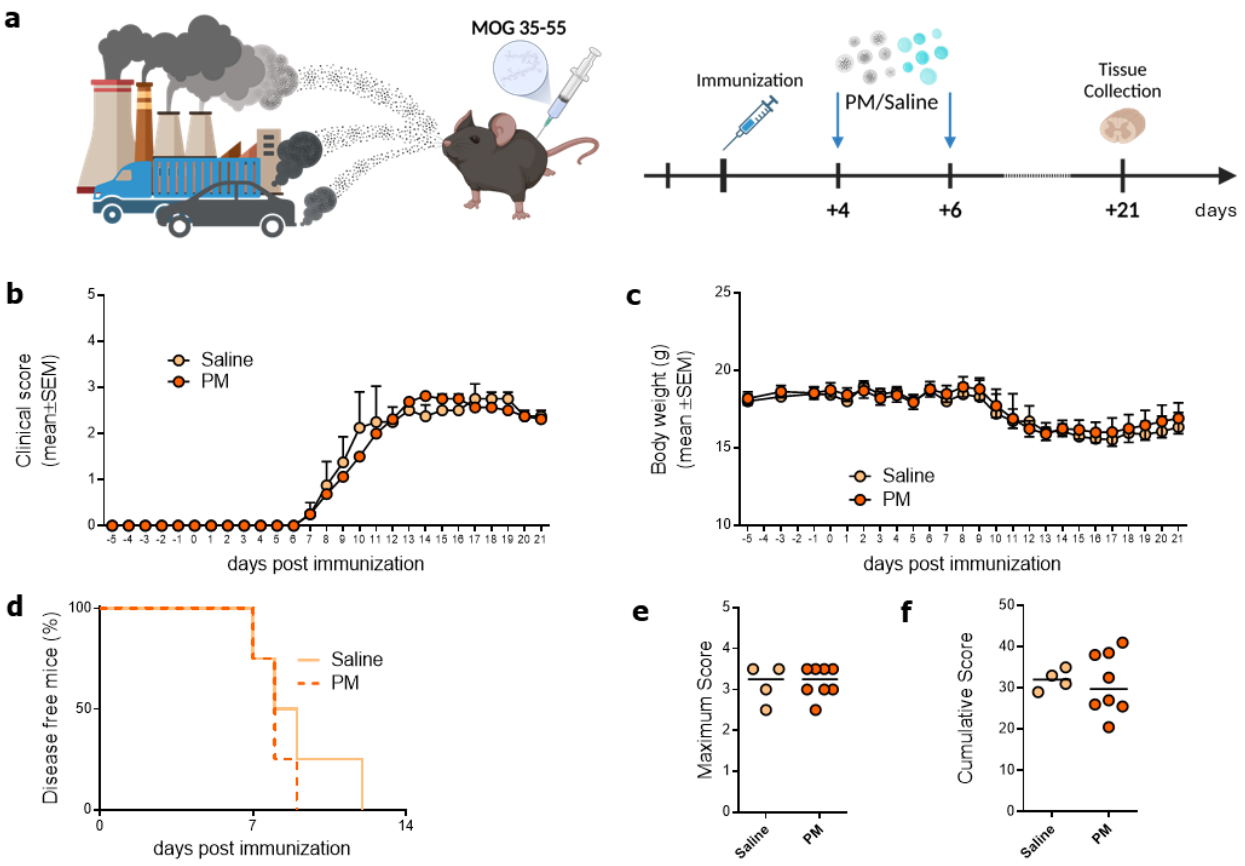

Figure 2 - Post-immunization exposure to PM_{10} does not alter EAE pathological course

(**a**) Schematic representation of the experiment design (graphics created with BioRender.com). (**b**) Mean clinical score of saline vs. PM_{10}-exposed EAE mice. (**c**) Mean body weight of saline vs. PM_{10}-exposed EAE mice during the pathological course. (**d**) Percentage of disease-free mice after EAE immunization. (**e**) Maximum clinical score reached by EAE mice during the pathological course. (**f**) Cumulative score obtained by saline or PM_{10}-exposed EAE mice in 21 days of assessment. Each dot in (**e,f**) represents an individual mouse. Source data are provided as a Source Data file (supplementary material).

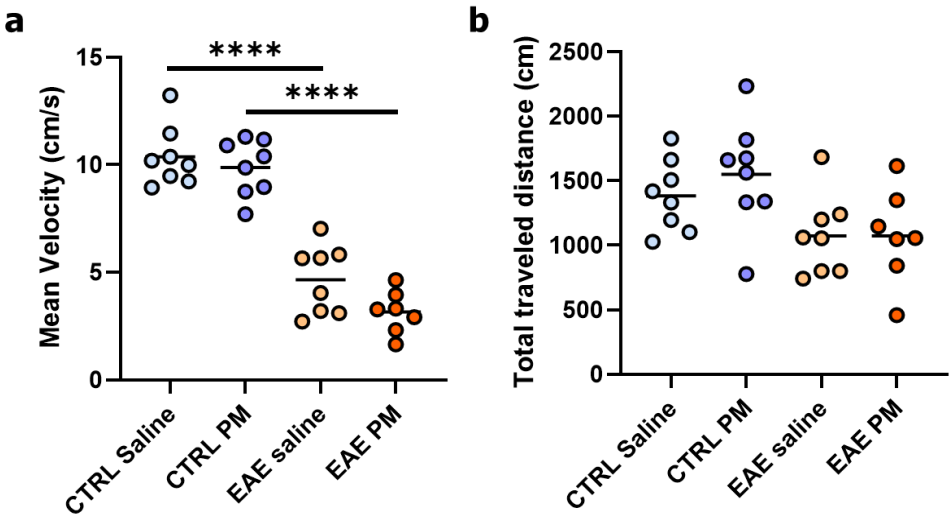

Supplementary Figure 1 - Additional behavioral analyses of Ctrl vs. EAE mice after acute PM_{10} exposure

(**a**) Mean speed of mice during the OF exploration. (**b**) Total distance traveled by mice during the EPM test. Each dot represents an individual mouse. Differences were assessed by Two-way ANOVA (see Suppl. Table 1 for P and F values of each comparison). *, P<0.05; **, P<0.01; ***, P<0.001. Source data are provided as a Source Data file (supplementary material).

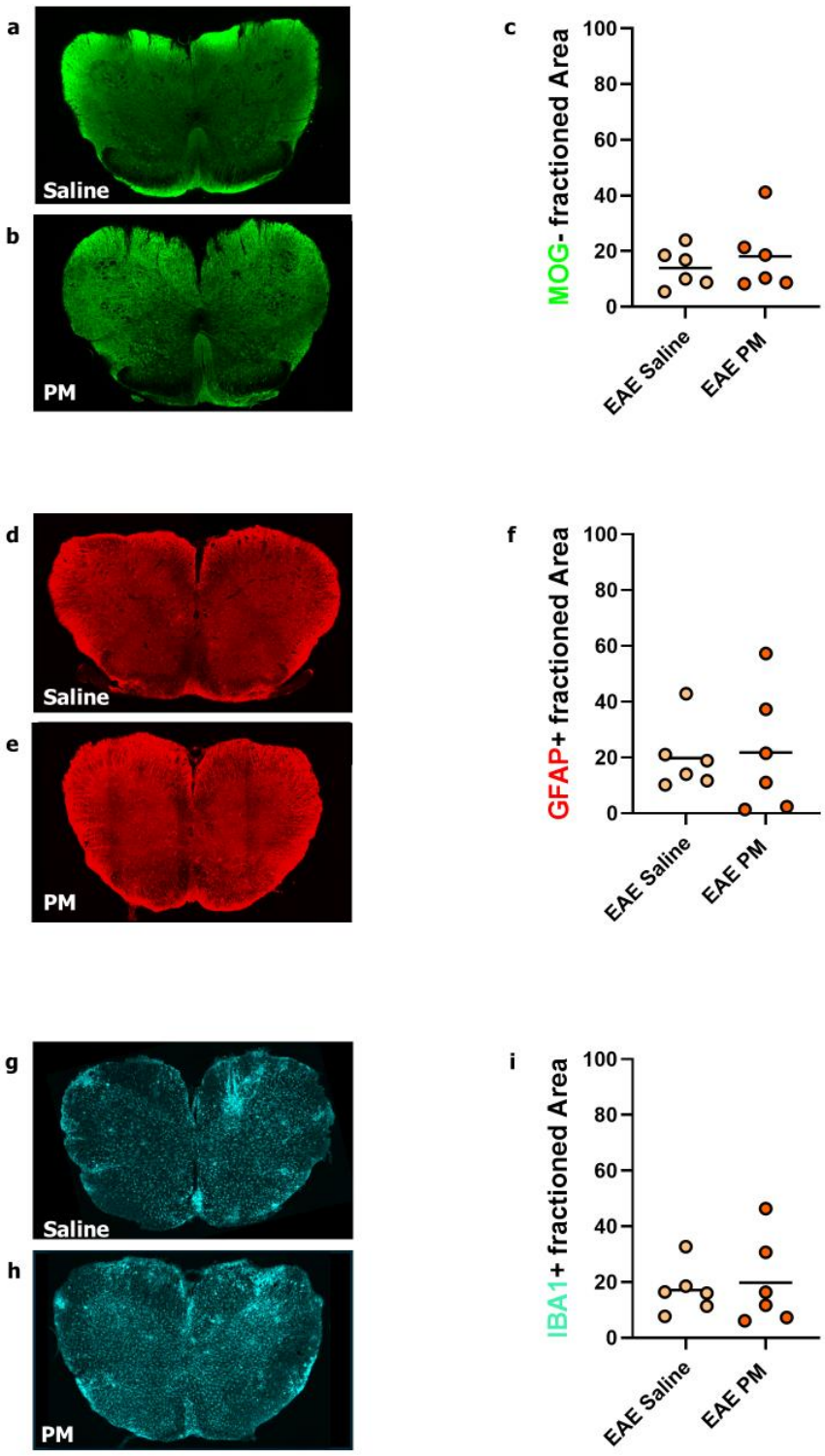

Figure 3 - Post-immunization exposure to PM_{10} does not alter EAE neuropathology

(**a,b**) Representative images of anti-MOG immunostaining in saline (**a**) and PM_{10}-exposed (**b**) EAE mouse lumbar spinal cord. (**c**) Quantification of the demyelinated (MOG-negative) area. (**d-e**) Representative images of anti-GFAP immunostaining in saline (**d**) and PM_{10}-exposed (**e**) EAE mouse lumbar spinal cord. (**f**) Quantification of GFAP+ area. (**g-h**) Representative images of IBA1 staining in saline (**g**) and PM_{10}-exposed (**h**) EAE mouse lumbar spinal cord. (**i**) Quantification of IBA1+ area. Each dot in (**c,f,i**) represents an individual mouse. Source data are provided as a Source Data file (supplementary material).

Acute exposure to PM_{10} selectively induces behavioral alterations in presymptomatic EAE mice

The Open Field (OF) test was performed to evaluate the gross motor function and emotional state (i.e. possible signs of anxiety) of EAE *vs.* healthy (Ctrl) mice early (i.e. 6h) after PM_{10} exposure (Fig. 4**a-d**). EAE mice exhibited a strong decrease in the total traveled distance (Fig. 4**c**) and mean speed (Supplementary Fig.1**a**), compared to Ctrl mice, in line with an early impairment of motor functions that could not be detected in the conventional clinical score assessment (see above and Fig.2). Exposure to PM_{10} did not have a significant effect on these parameters in both EAE and Ctrl mice (Fig. 4**c** and Supplementary Fig.1**a**). Yet, the tracking analysis - which distinguishes the central (i.e. distance traveled in the central part of the arena) *vs*. side (i.e. distance traveled in the "safer" space close to the walls of the arena) paths – detected a significant increase in the preference for the center in EAE mice exposed to PM_{10} compared to Ctrl and saline-exposed EAE mice (Fig. 4**d**), in line with a specific response of EAE mice to PM_{10} manifesting as a risk-taking and disinhibited behavior. To corroborate this interpretation and assess mouse predisposition to risk-taking *vs.* self-protective behaviors, we performed the Elevated Plus Maze (EPM) test (Fig. 4**e-g**). Consistent with the reduced motility observed in the OF test, both PM_{10}- and saline-exposed EAE groups displayed a reduced number of total entries in the arms of the EPM platform (Fig. 4**f**) as well as a reduced traveled distance compared to Ctrl mice (Supplementary Fig.1**b**). Yet, EAE mice exposed to PM_{10} showed an increased number of entries in the open arms of the EPM platform, compared to the other groups (Fig. 4**g**), in line with an increased risk-taking behavior. We then employed a modified Novel Object Location (NOL) test (in which the inter-trial interval was kept at 10 minutes) to assess novelty seeking behaviors (Fig. 4**h-k**). While both EAE mouse groups moved significantly less than Ctrl mice (as assessed by measuring the time spent exploring objects and the total traveled distance; Fig. 4**i,j**), EAE mice exposed to PM_{10} selectively showed an increased exploration of the displaced object during the second trial of the test (Fig. 4**k**), indicating an increased interest toward novelty.

To explore a possible interaction of PM exposure and EAE in the regulation of emotional behaviors, we performed the Tail Suspension Test (TST) as a measure of depressive symptoms (Fig. 4**l-n**). While both groups of EAE mice displayed a slight decrease in the percentage of time spent in immobility - maybe due to a higher susceptibility to discomfort (Fig. **4m**) - exposure to PM_{10} did not alter mouse behavior in the TST in both Ctrl and EAE mice (Fig. 4**m**,**n**). Finally, as possible indications of stress responses, we evaluated mouse stereotypic behaviors during free exploration in the OF (Fig. 4**o-t**). Decreased grooming events (Fig. 4**q**) and rearing time/events (Fig. 4**s,t**) were observed in EAE mice, in line with their reduced motility reported in other tests (see above). Yet, exposure to PM_{10} did not trigger any alteration in stereotypic behaviors in both Ctrl and EAE mouse groups (Fig. 4**p,q,s,t**).

Overall, results obtained from mouse phenotypic characterization converge in highlighting a specific vulnerability of EAE mice toward PM_{10}-induced behavioral alterations – presenting as increased risk-taking, disinhibited and novelty-seeking behaviors.

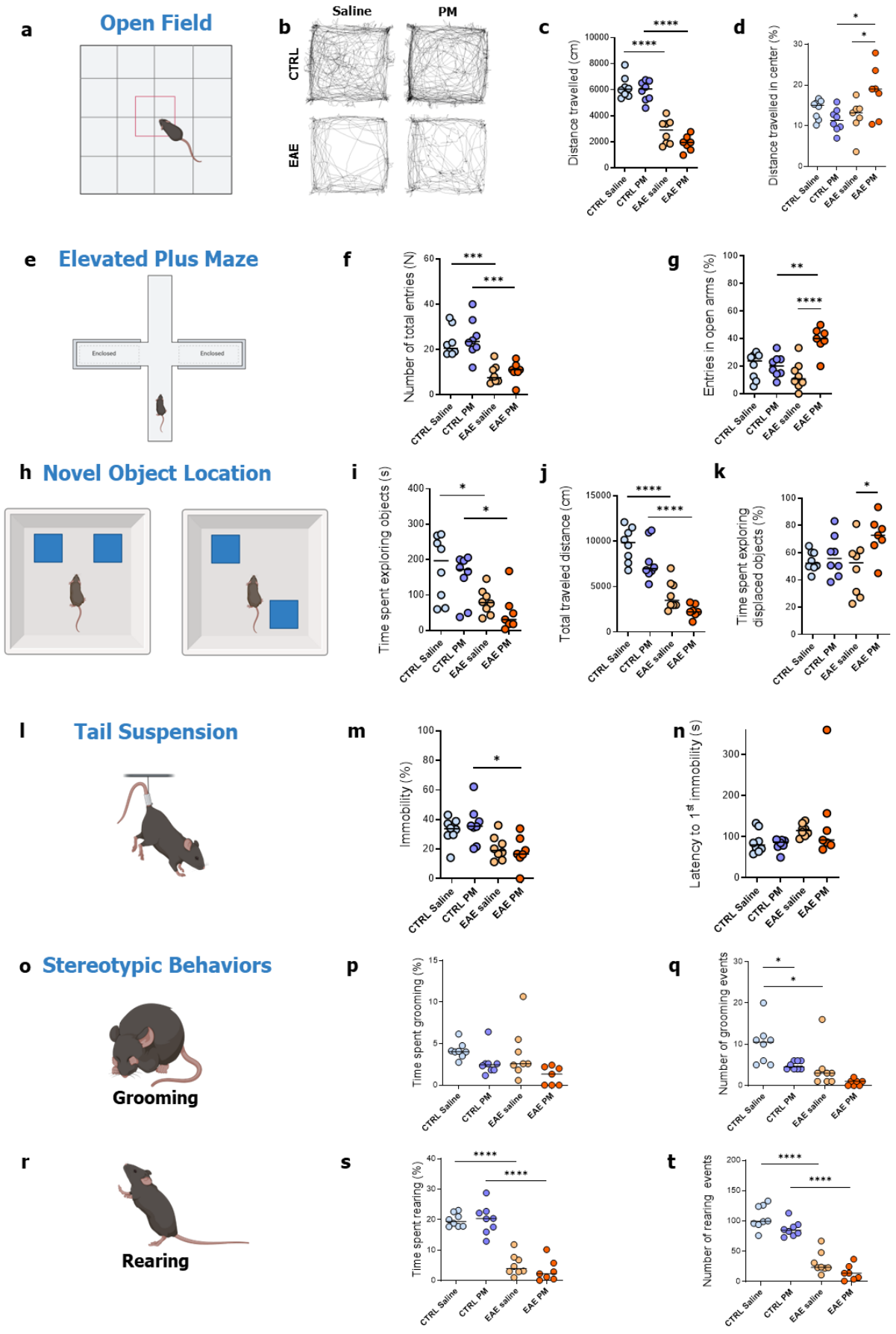

Figure 4 - Behavioral alterations elicited in presymptomatic EAE mice after acute PM_{10} exposure

(**a**) Schematic representation of the Open Field (OF) Test. (**b**) Plot tracks of the mouse paths in the OF arena after saline or PM_{10} exposure. (**c**) Total distance traveled by mice during the OF test. (**d**) Percentage of distance traveled in the central part of the OF arena during the test. (**e**) Schematic representation of the Elevated Plus Maze (EPM) test. (**f**) Total number of entries in arms during the EPM test. (**g**) Percentage of entries in open arms during the EPM test. (**h**) Schematic representation of the Novel Object Location (NOL) test. (**i**) Total time spent exploring objects in the NOL test. (**j**) Distance traveled during both trials of the NOL test. (**k**) Percentage of time spent exploring the displaced object in the NOL test. (**l**) Schematic representation of the Tail Suspension test. (**m**) Percentage of time spent in immobility during the TST. (**n**) Latency to first immobility during the TST. (**o**) Schematic representation of the grooming. (**p**) Percentage of total time spent grooming during the OF test. (**q**) Total number of grooming events during the OF test. (**r**) Schematic representation of the rearing. (**s**) Percentage of time spent rearing during the OF test. (**t**) Total number of rearing events during the OF test. Each dot represents an individual mouse. In all instances, differences among groups have been evaluated by means of the Two-ways Anova test followed by Bonferroni's post-hoc analysis (n, P, and F values in Supplementary Table 1). Statistical differences were indicated with * $P < 0.05$, ** $P < 0.01$, *** $P < 0.001$, **** $P < 0.0001$. Source data are provided as a Source Data file. Graphics created with BioRender.com.

Acute exposure to PM_{10} does not alter dopamine availability or dopamine system gene expression in the brain of EAE mice

To assess the biological substrate of the selective response elicited in EAE mice by PM_{10}, we reasoned to investigate possible changes of the dopaminergic neurotransmission, which were formerly associated with increased impulsive, risk-taking and novelty-seeking behaviors and alterations in spontaneous locomotion and stereotypic behaviors (Pogorelov et al., 2005; Kalueff et al., 2016; see also Discussion). Brain dopamine levels tended to increase in both EAE groups compared to Ctrl mice as well as in PM_{10}-exposed Ctrl mice compared to saline-exposed Ctrl mice, as assessed by HPLC analysis (Fig. 5**a**). Yet, no significant change in dopamine was found associated with PM_{10} exposure in EAE mice (Fig. 5**a**). We then looked for possible changes in the expression of genes coding for dopamine receptors, transporters and synthetic/degrading enzymes (Fig. 5**b** and Supplementary Fig. 2), that might be at base of the different behavioral response of EAE mice to PM_{10}. Drd1, Drd2 (coding for the dopamine receptors 1 and 2) and Vps35 (coding for the vacuolar protein sorting-35, involved the dopamine transporter endosomal recycling) transcripts appeared decreased in EAE mice, whereas no significant change in gene expression was detected as associated with PM_{10} exposure in both Ctrl and EAE mice (Fig. 5**b** and Supplementary Fig. 2).

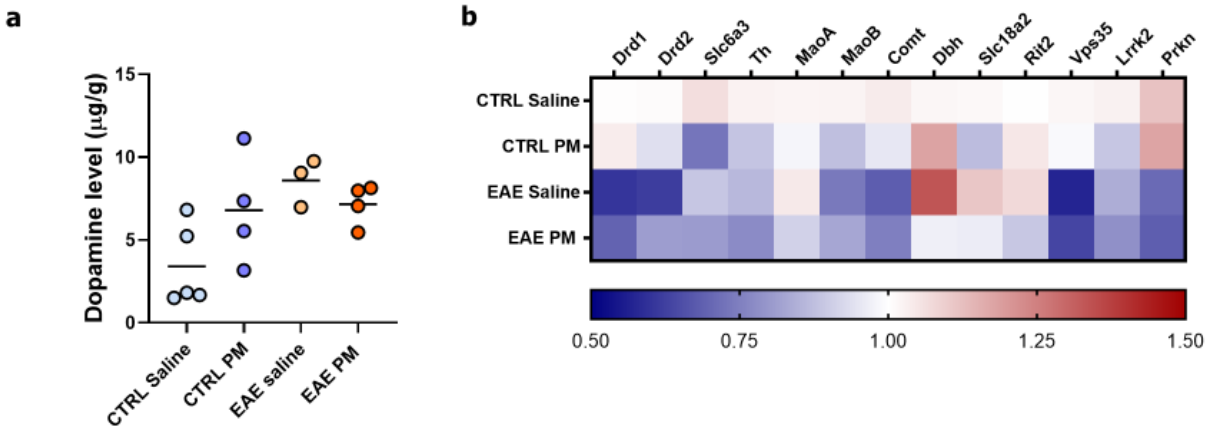

Figure 5 - Dopamine availability and expression of dopamine system genes are not altered by exposure to PM_{10}

(**a**) Quantification of dopamine by HPLC in the mouse brain tissue. (**b**) Heatmap of the qRT-PCR analysis of dopamine system gene expression. Two-way Anova followed by Bonferroni's Multiple Comparison Test (n, P, and F values in Supplementary Table 1). Dot plots of the represented data are included in Supplementary Fig 2. Source data are provided as a Source Data file (supplementary material).

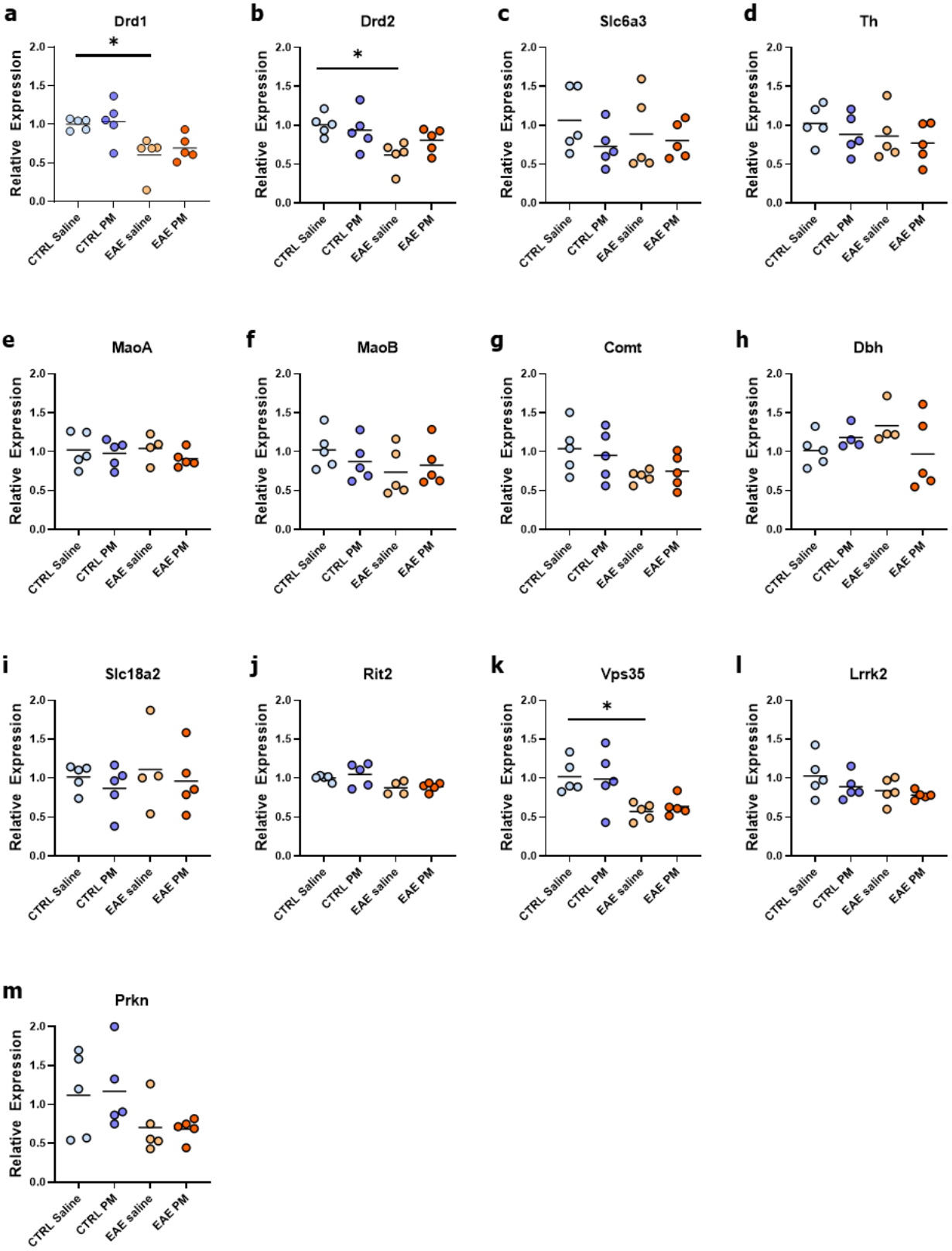

Supplementary Figure 2 - qRT-PCR expression analysis in mouse forebrain.

Dot plots referring to Figure 5**b**. Each dot represents an individual mouse. Differences were assessed by Two-way ANOVA (see Suppl. Table 1 for P and F values of each comparison). *, P<0.05; **, P<0.01; ***, P<0.001, ****P < 0.0001. Source data are provided as a Source Data file.

Discussion

Epidemiological studies have shown that transient increases of airborne PM (i.e. PM peaks) are associated with higher rates of hospitalization for MS onset or relapses, and exacerbation of neuroinflammation in MS patients[3-9]. This prompted the hypothesis that even short-term exposures to high concentrations of PM may contribute to MS emergence in predisposed subjects or trigger relapses in people with MS. To tackle this issue, we combined an immune priming against myelin antigens (i.e. the induction of chronic EAE, the most common animal model of MS; Procaccini et al., 2015) in the mouse with the acute exposure to $PM_{10,}$ either before the immunization or during the pre-symptomatic phase of the EAE course. Although acute PM_{10} exposures did not significantly influence the onset time or the severity of EAE in terms of mouse motor impairment (i.e. clinical score) and neuropathology, presymptomatic EAE mice showed behavioral alterations early after being exposed to PM_{10}. Specifically, increased disinhibited, risk-taking and novelty-seeking behaviors were triggered 6 hours after exposure to PM_{10} in EAE – but not healthy mice - in line with a specific vulnerability of immunologically primed mice toward the effects of PM well before the emergence of overt functional impairment.

Besides motor, sensory and autonomic disturbances, cognitive and psychiatric symptoms are common in people with MS and have an important impact on their quality of life and daily activities (including fatigue or even adherence to therapy; Benedict et al., 2020; Sparaco et al., 2021). While in most cases such disturbances fall in the memory/speed processing and depression/anxiety domains, deficits of attention, impulsivity and alteration of decision-making abilities have been also reported in people with MS (Paul et al., 1998; Toro et al., 2018; Neuhaus et al., 2018). Of note, cognitive impairment can be detected even in the early stages of MS and tobacco smoking - one the major source of indoor PM pollution (Ni et al., 2020) - was recognized as one of the most influential risk factors for worse cognition in early MS (McNicholas et al., 2017). Thus, it would be interesting to assess whether, similar to what was observed in presymptomatic EAE mice, exposure to PM might be associated with increased impulsivity, emergence/worsening of attention deficits or behavior/mood alterations in people with MS, thereby unveiling an additional aspect of vulnerability to PM in the cohort of MS patients.

Notably, while most people can homeostatically cope with the negative effects of PM exposure, more vulnerable cohorts exist that show an increased sensitivity toward the consequences of PM exposure. Such susceptibility relies on genetic or acquired factors that make the biological responses triggered by PM different compared to those activated in healthy subjects (Hooper and Kaufman, 2018). The specific nature, timing and selective occurrence of PM-induced behavioral alterations in EAE - but not in healthy - mice, prompted the hypothesis that their biological basis might reside in the interaction of PM-elicited events with an already dysregulated neurotransmitter setting - perhaps

consequent to immune priming - in EAE mouse CNS (Akyuz et al., 2023). Among neurotransmitters, we opted for analyzing the possible involvement of the dopamine system for a number of reasons. First, in Dat1 hemizygous mice, reduced expression of the dopamine transporter DAT - the primary mechanism for dopamine clearance after release at synapse - resulted in risk-taking and novelty-seeking behaviors reminiscent of those observed in PM_{10}-exposed EAE mice (Pogorelov et al., 2005). Dopamine is also a crucial modulator in the regulation of spontaneous locomotion and stereotypic behaviors, such as grooming (Kalueff et al., 2016). As relevant for MS, dopamine imbalance has been proposed as a substrate of the cognitive fatigue in MS patients (Dobryakova et al., 2015), whereas alterations of dopamine neurotransmission and an imbalance between DR1 *vs.* DR2 receptor signaling were reported as associated with low-grade inflammation in EAE mice (Gentile et al., 2014). Finally, former studies showed that exposure to ambient PM decreased dopamine uptake in the rat striatum (Andrade-Oliva et al., 2023), whereas exposure to PM extracted from tobacco combustion resulted in a rapid (as early as 1 hour after treatment) decrease of Dat mRNA in the ventral tegmental area and altered DAT function in the dorsal striatum of rats (Danielson et al., 2014). Yet, in contrast to our expectations, although dopamine tended to increase in the brain of EAE compared to Ctrl mice and in PM_{10}-exposed compared to saline-exposed Ctrl mice, no significant change in dopamine was detected in association with PM_{10}-exposure in EAE mice. Moreover, besides a basal reduction of Drd1, Drd2 and Vps35 mRNAs in EAE vs. Ctrl mice, no significant change in the expression of transcripts coding for dopamine receptors, transporters or biosynthetic/degrading enzymes was detected in either EAE *vs.* Ctrl mice or in PM_{10}-exposed *vs.* saline-exposed EAE mice. These findings may suggest the involvement of alternative mechanistic substrates. Yet, since our analysis was performed on whole brain tissue extracts, we cannot exclude that region-specific alterations in dopamine availability or in the expression of dopamine signaling mediators/modulators might be present although not detected in our quantifications.

In conclusion, our study unveils a specific vulnerability of EAE mice toward PM_{10}-induced behavioral alterations even before they manifest overt neuropathological signs, in line with the idea that the immunological background of the subjects influences the outcome of PM_{10} exposure and pointing to immunologically primed individuals - such as people with MS - as a vulnerable population cohort toward the effects of air pollution.

Author contributions

MB, FM: Data curation, Formal analysis, Investigation, Methodology, Visualization, Writing – original draft, Writing –review & editing.

RP, SDF, NDC, CP: Data curation, Formal analysis, Investigation, Methodology, Writing –review & editing.

AB, AB: Conceptualization, Writing –review & editing.

EB: Conceptualization, Data curation, Formal analysis, Visualization, Writing – original draft, Writing – review & editing, Funding acquisition, Project administration, Supervision.

Data availability

All data are available in the main text or in the Source data file enclosed as supplementary material.

Declaration of competing interest

The authors declare no conflict of interest. The funding sponsors had no role in the interpretation of data or in the writing of the manuscript.

Acknowledgements

We wish to thank Dr. Marco Cambiaghi (Department of Neuroscience, Biomedicine and Movement Sciences, University of Verona, Italy) for precious help in NOL test analysis. Our work was supported by FISM - Fondazione Italiana Sclerosi Multipla (Italy) (ID:2019/PR-Multi/003) and by Cassa di Risparmio di Torino (CRT) Foundation grant (ID: 2021.0657) to EB. MB was supported by a PON R&I 2014-2020 PhD Fellowship “Dottorati di ricerca su tematiche green e dell’innovazione”, financed by Ministero dell’Istruzione, dell’Università e della Ricerca—MIUR (Italy) in the frame of FSE–REACT EU. This study was also supported by Ministero dell’Istruzione, dell’Università e della Ricerca—MIUR (Italy) project “Dipartimenti di Eccellenza 2018–2022” and “Dipartimenti di Eccellenza 2013–2027” to Dept. of Neuroscience “Rita Levi Montalcini” of the University of Turin.

References

Akhtar, U. S., McWhinney, R. D., Rastogi, N., Abbatt, J. P. D., Evans, G. J., & Scott, J. A. (2010). Cytotoxic and proinflammatory effects of ambient and source-related particulate matter (PM) in relation to the production of reactive oxygen species (ROS) and cytokine adsorption by particles. Inhalation Toxicology, 22(sup2), 37–47. https://doi.org/10.3109/08958378.2010.518377

Akyuz, E., Celik, B. R., Aslan, F. S., Sahin, H., & Angelopoulou, E. (2023). Exploring the role of Neurotransmitters in Multiple sclerosis: An expanded review. *ACS Chemical Neuroscience*, *14*(4), 527–553. https://doi.org/10.1021/acschemneuro.2c00589

Andrade-Oliva, M., Debray-García, Y., Morales-Figueroa, G., Escamilla-Sánchez, J., Amador-Muñoz, O., Díaz-Godoy, R. V., Kleinman, M., Florán, B., Arias-Montaño, J., & De Vizcaya-Ruiz, A. (2022). Effect of subchronic exposure to ambient fine and ultrafine particles on rat motor activity and ex vivo striatal dopaminergic transmission. *Inhalation Toxicology*, *35*(1–2), 1–13. https://doi.org/10.1080/08958378.2022.2140228

Angelici, L., Piola, M., Cavalleri, T., Randi, G., Cortini, F., Bergamaschi, R., Baccarelli, A. A., Bertazzi, P. A., Pesatori, A. C., & Bollati, V. (2016). Effects of particulate matter exposure on multiple sclerosis hospital admission in Lombardy region, Italy. Environmental Research, 145, 68–73. https://doi.org/10.1016/j.envres.2015.11.017

Babadjouni, R. M., Hodis, D. M., Radwanski, R., Durazo, R., Patel, A., Liu, Q., & Mack, W. J. (2017). Clinical effects of air pollution on the central nervous system; a review. Journal of Clinical Neuroscience, 43, 16–24. https://doi.org/10.1016/j.jocn.2017.04.028

Becker, S., Fenton, M. J., & Soukup, J. M. (2002). Involvement of microbial components and toll-like receptors 2 and 4 in cytokine responses to air pollution particles. American Journal of Respiratory Cell and Molecular Biology, 27(5), 611–618. https://doi.org/10.1165/rcmb.4868

Benedict, R. H. B., Amato, M. P., DeLuca, J., & Geurts, J. J. G. (2020). Cognitive impairment in multiple sclerosis: clinical management, MRI, and therapeutic avenues. The Lancet Neurology, 19(10), 860–871. https://doi.org/10.1016/s1474-4422(20)30277-5

Bergamaschi, R., Cortese, A., Pichiecchio, A., Berzolari, F. G., Borrelli, P., Mallucci, G., Bollati, V., Romani, A., Nosari, G., Villa, S., & Montomoli, C. (2017). Air pollution is associated to the multiple sclerosis inflammatory activity as measured by brain MRI. Multiple Sclerosis Journal, 24(12), 1578–1584. https://doi.org/10.1177/1352458517726866

Bergamaschi, R., & Montomoli, C. (2021). Air pollution is a risk factor for multiple sclerosis – Yes. Multiple Sclerosis Journal, 27(14), 2137–2138. https://doi.org/10.1177/13524585211035953

Boda, E., Hoxha, E., Pini, A., Montarolo, F., & Tempia, F. (2011). Brain expression of KV3 subunits during development, adulthood and aging and in a murine model of Alzheimer's disease. Journal of Molecular Neuroscience, 46(3), 606–615. https://doi.org/10.1007/s12031-011-9648-6

Boda, E., Rigamonti, A. E., & Bollati, V. (2020). Understanding the effects of air pollution on neurogenesis and gliogenesis in the growing and adult brain. Current Opinion in Pharmacology, 50, 61–66. https://doi.org/10.1016/j.coph.2019.12.003

Boda, E., Lorenzati, M., Parolisi, R., Harding, B., Pallavicini, G., Bonfanti, L., Moccia, A., Bielas, S., Di Cunto, F., & Buffo, A. (2022). Molecular and functional heterogeneity in dorsal and ventral

oligodendrocyte progenitor cells of the mouse forebrain in response to DNA damage. Nature Communications, 13(1). https://doi.org/10.1038/s41467-022-30010-6

Butts, B. D., Houde, C., & Mehmet, H. (2008). Maturation-dependent sensitivity of oligodendrocyte lineage cells to apoptosis: implications for normal development and disease. Cell Death and Differentiation, 15(7), 1178–1186. https://doi.org/10.1038/cdd.2008.70

Calderón-Garcidueñas, L., Solt, A. C., Henríquez-Roldán, C., Torres-Jardón, R., Nuse, B., Herritt, L., Villarreal-Calderón, R., Osnaya, N., Stone, I., García, R., Brooks, D. M., González-Maciel, A., Reynoso-Robles, R., Delgado-Chávez, R., & Reed, W. (2008). Long-term Air Pollution Exposure Is Associated with Neuroinflammation, an Altered Innate Immune Response, Disruption of the Blood-Brain Barrier, Ultrafine Particulate Deposition, and Accumulation of Amyloid β-42 and α-Synuclein in Children and Young Adults. Toxicologic Pathology, 36(2), 289–310. https://doi.org/10.1177/0192623307313011

Calderón-Garcidueñas, L., Kulesza, R. J., Doty, R. L., D'Angiulli, A., & Torres-Jardón, R. (2015). Megacities air pollution problems: Mexico City Metropolitan Area critical issues on the central nervous system pediatric impact. Environmental Research, 137, 157–169. https://doi.org/10.1016/j.envres.2014.12.012

Christensen, L. B., Woods, T. A., Carmody, A. B., Caughey, B., & Peterson, K. E. (2014). Age-related differences in neuroinflammatory responses associated with a distinct profile of regulatory markers on neonatal microglia. Journal of Neuroinflammation, 11(1). https://doi.org/10.1186/1742-2094-11-70

Cortese, A., Lova, L., Comoli, P., Volpe, E., Villa, S., Mallucci, G., La Salvia, S., Romani, A., Franciotta, D., Bollati, V., Basso, S., Guido, I., Quartuccio, G., Battistini, L., Cereda, C., & Bergamaschi, R. (2020). Air pollution as a contributor to the inflammatory activity of multiple sclerosis. Journal of Neuroinflammation, 17(1). https://doi.org/10.1186/s12974-020-01977-0

Danielson, K., Putt, F., Truman, P., & Kivell, B. M. (2013). The effects of nicotine and tobacco particulate matter on dopamine uptake in the rat brain. *Synapse*, *68*(2), 45–60. https://doi.org/10.1002/syn.21715

Dobryakova, E., Genova, H. M., DeLuca, J., & Wylie, G. R. (2015). The dopamine imbalance hypothesis of fatigue in multiple sclerosis and other neurological disorders. *Frontiers in Neurology*, *6*. https://doi.org/10.3389/fneur.2015.00052

Ebers, G. C. (2008). Environmental factors and multiple sclerosis. The Lancet Neurology, 7(3), 268–277. https://doi.org/10.1016/s1474-4422(08)70042-5

Franklin, R. J. M., & Ffrench-Constant, C. (2008). Remyelination in the CNS: from biology to therapy. Nature Reviews. Neuroscience, 9(11), 839–855. https://doi.org/10.1038/nrn2480

Fumagalli, M., Lombardi, M., Gressens, P., & Verderio, C. (2018). How to reprogram microglia toward beneficial functions. Glia, 66(12), 2531–2549. https://doi.org/10.1002/glia.23484

Gałuszka-Bulaga, A., Tkacz, K., Węglarczyk, K., Siedlar, M., & Baran, J. (2023). Air pollution induces pyroptosis of human monocytes through activation of inflammasomes and Caspase-3-dependent pathways. Journal of Inflammation, 20(1). https://doi.org/10.1186/s12950-023-00353-y

Gawda, A., Majka, G., Nowak, B., & Marcinkiewicz, J. (2017). Air pollution, oxidative stress, and exacerbation of autoimmune diseases. Central European Journal of Immunology, 3, 305–312. https://doi.org/10.5114/ceji.2017.70975

Gentile, A., Fresegna, D., Federici, M., Musella, A., Rizzo, F. R., Sepman, H., Bullitta, S., De Vito, F., Haji, N., Rossi, S., Mercuri, N. B., Usiello, A., Mandolesi, G., & Centonze, D. (2015). Dopaminergic dysfunction is associated with IL-1β-dependent mood alterations in experimental autoimmune encephalomyelitis. *Neurobiology of Disease*, *74*, 347–358. https://doi.org/10.1016/j.nbd.2014.11.022

Gómez-Budia, M., Konttinen, H., Saveleva, L., Korhonen, P., Jalava, P. I., Kanninen, K. M., & Malm, T. (2020). Glial smog: Interplay between air pollution and astrocyte-microglia interactions. Neurochemistry International, 136, 104715. https://doi.org/10.1016/j.neuint.2020.104715

Gregory, A. C., Shendell, D. G., Okosun, I. S., & Gieseker, K. E. (2008). Multiple Sclerosis disease distribution and potential impact of environmental air pollutants in Georgia. The Science of the Total Environment, 396(1), 42–51. https://doi.org/10.1016/j.scitotenv.2008.01.065

Han, B., Li, X., Ai, R., Deng, S., Ye, Z., Deng, X., Ma, W., Xiao, S., Wang, J., Wang, L., Xie, C., Zhang, Y., Xu, Y., & Zhang, Y. (2022). Atmospheric particulate matter aggravates CNS demyelination through involvement of TLR-4/NF-kB signaling and microglial activation. eLife, 11. https://doi.org/10.7554/elife.72247

Heydarpour, P., Amini, H., Khoshkish, S., Seidkhani, H., Sahraian, M. A., & Yunesian, M. (2014). Potential impact of air pollution on multiple sclerosis in Tehran, Iran. Neuroepidemiology, 43(3–4), 233–238. https://doi.org/10.1159/000368553

Hooper, L. G., & Kaufman, J. D. (2018). Ambient air pollution and clinical implications for susceptible populations. *Annals of the American Thoracic Society*, *15*(Supplement_2), S64–S68. https://doi.org/10.1513/annalsats.201707-574mg

Jeanjean, M., Bind, M., Roux, J., Ongagna, J., De Sèze, J., Bard, D., & Leray, E. (2018). Ozone, NO2 and PM10 are associated with the occurrence of multiple sclerosis relapses. Evidence from seasonal multi-pollutant analyses. Environmental Research, 163, 43–52. https://doi.org/10.1016/j.envres.2018.01.040

Kalueff, A. V., Stewart, A. M., Song, C., Berridge, K. C., Graybiel, A. M., & Fentress, J. C. (2015). Neurobiology of rodent self-grooming and its value for translational neuroscience. *Nature Reviews. Neuroscience*, *17*(1), 45–59. https://doi.org/10.1038/nrn.2015.8

Kewcharoenwong, C., Khongmee, A., Nithichanon, A., Palaga, T., Prueksasit, T., Mudway, I. S., Hawrylowicz, C. M., & Lertmemongkolchai, G. (2023). Vitamin D3 regulates PM-driven primary human neutrophil inflammatory responses. Scientific Reports, 13(1). https://doi.org/10.1038/s41598-023-43252-1

Klocke, C., Allen, J. L., Sobolewski, M., Blum, J. L., Zelikoff, J. T., & Cory-Slechta, D. A. (2018). Exposure to fine and ultrafine particulate matter during gestation alters postnatal oligodendrocyte maturation, proliferation capacity, and myelination. NeuroToxicology, 65, 196–206. https://doi.org/10.1016/j.neuro.2017.10.004

Lemprière, S. (2020). Air pollution linked to multiple sclerosis and stroke. Nature Reviews Neurology, 16(3), 127. https://doi.org/10.1038/s41582-020-0322-x

McNicholas, N., O'Connell, K., Yap, S. M., Killeen, R. P., Hutchinson, M., & McGuigan, C. (2017). Cognitive dysfunction in early multiple sclerosis: a review. QJM, 111(6), 359–364. https://doi.org/10.1093/qjmed/hcx070

Montarolo, F., Perga, S., Martire, S., & Bertolotto, A. (2015). Nurr1 reduction influences the onset of chronic EAE in mice. Inflammation Research, 64(11), 841–844. https://doi.org/10.1007/s00011-015-0871-4

Montarolo, F., Martire, S., Chiara, F., Allegra, S., De Francia, S., Hoxha, E., Tempia, F., Capobianco, M.A., Bertolotto, A. (2022). NURR1-deficient mice have age- and sex-specific behavioral phenotypes. J Neurosci Res. 100(9), 1747-1754 . https://doi.org/10.1002/jnr.25067.

Nejad, S. H., Takechi, R., Mullins, B. J., Giles, C., Larcombe, A. N., Bertolatti, D., Rumchev, K., Dhaliwal, S., & Mamo, J. (2014). The effect of diesel exhaust exposure on blood–brain barrier integrity and function in a murine model. Journal of Applied Toxicology, 35(1), 41–47. https://doi.org/10.1002/jat.2985

Neuhaus, M., Calabrese, P., & Annoni, J. (2018). Decision-Making in Multiple sclerosis Patients: A Systematic review. Multiple Sclerosis International, 2018, 1–9. https://doi.org/10.1155/2018/7835952

Ni, Y., Shi, G., & Qu, J. (2020). Indoor PM2.5, tobacco smoking and chronic lung diseases: A narrative review. Environmental Research, 181, 108910. https://doi.org/10.1016/j.envres.2019.108910

Noorimotlagh, Z., Azizi, M., Pan, H., Mami, S., & Mirzaee, S. A. (2021). Association between air pollution and Multiple Sclerosis: A systematic review. Environmental Research, 196, 110386. https://doi.org/10.1016/j.envres.2020.110386

Oikonen, M., Laaksonen, M., Laippala, P., Oksaranta, O., Lilius, E., Lindgren, S., Rantio-Lehtimäki, A., Anttinen, A., Koski, K., & Erälinna, J. (2003). Ambient air quality and occurrence of multiple sclerosis relapse. Neuroepidemiology, 22(1), 95–99. https://doi.org/10.1159/000067108

Park, Y., Lee, I., Lee, M. J., Park, H., Jung, G. S., Kim, N., Im, W., Kim, H., Lee, J. H., Cho, S., & Choi, Y. S. (2024). Particulate matter exposure induces adverse effects on endometrium and fertility via aberrant inflammatory and apoptotic pathways in vitro and in vivo. Chemosphere, 361, 142466. https://doi.org/10.1016/j.chemosphere.2024.142466

Parolisi, R., Montarolo, F., Pini, A., Rovelli, S., Cattaneo, A., Bertolotto, A., Buffo, A., Bollati, V., & Boda, E. (2021). Exposure to fine particulate matter (PM2.5) hampers myelin repair in a mouse model of white matter demyelination. Neurochemistry International, 145, 104991. https://doi.org/10.1016/j.neuint.2021.104991

Paul, R. H., Beatty, W. W., Schneider, R., Blanco, C., & Hames, K. (1998). Impairments of attention in individuals with Multiple Sclerosis. Multiple Sclerosis Journal, 4(5), 433–439. https://doi.org/10.1177/135245859800400506

Peeples, L. (2020). How air pollution threatens brain health. Proceedings of the National Academy of Sciences, 117(25), 13856–13860. https://doi.org/10.1073/pnas.2008940117

Pogorelov, V. M., Rodriguiz, R. M., Insco, M. L., Caron, M. G., & Wetsel, W. C. (2005). Novelty Seeking and Stereotypic Activation of Behavior in Mice with Disruption of the Dat1 Gene. *Neuropsychopharmacology*, *30*(10), 1818–1831. https://doi.org/10.1038/sj.npp.1300724

Procaccini, C., De Rosa, V., Pucino, V., Formisano, L., & Matarese, G. (2015). Animal models of Multiple Sclerosis. European Journal of Pharmacology, 759, 182–191. https://doi.org/10.1016/j.ejphar.2015.03.042

Roux, J., Bard, D., Pabic, E. L., Segala, C., Reis, J., Ongagna, J., De Sèze, J., & Leray, E. (2017). Air pollution by particulate matter PM10 may trigger multiple sclerosis relapses. Environmental Research, 156, 404–410. https://doi.org/10.1016/j.envres.2017.03.049

Sellner, J., Kraus, J., Awad, A., Milo, R., Hemmer, B., & Stüve, O. (2011). The increasing incidence and prevalence of female multiple sclerosis—A critical analysis of potential environmental factors. Autoimmunity Reviews, 10(8), 495–502. https://doi.org/10.1016/j.autrev.2011.02.006

Sierra-Vargas, M. P., & Teran, L. M. (2012). Air pollution: Impact and prevention. Respirology, 17(7), 1031–1038. https://doi.org/10.1111/j.1440-1843.2012.02213.x

Sparaco, M., Lavorgna, L., & Bonavita, S. (2019). Psychiatric disorders in multiple sclerosis. Journal of Neurology, 268(1), 45–60. https://doi.org/10.1007/s00415-019-09426-6

Toro, J., Blanco, L., Orozco-Cabal, L. F., Díaz, C., Reyes, S., Burbano, L., Cuéllar-Giraldo, D. F., Duque, A., Patiño, J., & Cortés, F. (2018). Impulsivity traits in patients with multiple sclerosis. Multiple Sclerosis and Related Disorders, 22, 148–152. https://doi.org/10.1016/j.msard.2018.04.011

Woo, M. S., Engler, J. B., & Friese, M. A. (2024). The neuropathobiology of multiple sclerosis. Nature Reviews. Neuroscience, 25(7), 493–513. https://doi.org/10.1038/s41583-024-00823-z

Woodward, N. C., Pakbin, P., Saffari, A., Shirmohammadi, F., Haghani, A., Sioutas, C., Cacciottolo, M., Morgan, T. E., & Finch, C. E. (2017). Traffic-related air pollution impact on mouse brain accelerates myelin and neuritic aging changes with specificity for CA1 neurons. Neurobiology of Aging, 53, 48–58. https://doi.org/10.1016/j.neurobiolaging.2017.01.007

Žibert, J., Cedilnik, J., & Pražnikar, J. (2016). Particulate matter (PM10) patterns in Europe: An exploratory data analysis using non-negative matrix factorization. Atmospheric Environment, 132, 217–228. https://doi.org/10.1016/j.atmosenv.2016.03.005

Supplementary Table 1 - Statistical Analyses

Figure	Applied Test	n	P value	Statistics	Post hoc analyses	Post hoc results
1b	Two-way Anova	n=10	Time Effect: P<0,0001 Exposure Effect: P=0,2616 Time x Exposure: P=0,9514	Time: F (24, 528) = 62,09 Exposure: F (1, 22) = 1,328 Time x Exposure: F (24, 528) = 0,5699	Bonferroni's Multiple Comparisons Test	
1c	Two-way Anova	Saline=10 PM=14	Time Effect: P<0,0001 Exposure Effect: P=0,4656 Time x Exposure: P=0,9982	Time: F (24, 525) = 14,57 Exposure: F (1, 22) = 0,5513 Time x Exposure: F (24, 525) = 0,3568	Bonferroni's Multiple Comparisons Test	
1d	Kaplan-Meier	Saline=10 PM=14	n.s.			
1e	Mann Whitney test (two tailed)	Saline=10 PM=14	n.s.			
1f	Mann Whitney test (two tailed)	Saline=10 PM=14	n.s.			
2b	Two-way Anova	Saline=4 PM=8	Time Effect: P<0,0001 Exposure Effect: P=0,8277 Time x Exposure: P= 0,9994	Time: F (26, 260) = 46,49 Exposure: F (1, 10) = 0,04993 Time x Exposure: F (26, 260) = 0,3242	Bonferroni's Multiple Comparisons Test	
2c	Two-way Anova	Saline=4 PM=8	Time Effect: P<0,0001	Time: F (24, 240) = 10,10	Bonferroni's Multiple Comparisons Test	

			Exposure Effect: P=0,7801 Time x Exposure: P>0,9999	Exposure: F (1, 10) = 0,08229 Time x Exposure: F (24, 240) = 0,1911		
2d	Kaplan-Meier	Saline=4 PM=8	n.s.			
2e	Unpaired t test (two tailed)	Saline=4 PM=8	n.s.			
2f	Unpaired t test (two tailed)	Saline=4 PM=8	n.s.			
3c	Unpaired t test (two tailed)	n=6	n.s.			
3f	Unpaired t test (two tailed)	n=6	n.s.			
3i	Unpaired t test (two tailed)	n=6	n.s.			
4c	Two-way Anova	CTRL Saline = 8 CTRL PM = 8 EAE Saline = 8 EAE PM = 7	Immunization Effect: P <0,0001 Exposure Effect: P= 0,0518 Immunization x Exposure: P= 0,3011	Immunization: F(1, 27) = 164,0 Exposure: F(1, 27) = 4,140 Immunization x Exposure: F (1, 27) = 1,112	Bonferroni's Multiple Comparisons Test	CTRL Sal. vs CTRL PM: n.s. CTRL Sal. vs EAE Sal.: P<0,0001 CTRL PM vs EAE PM: P<0,0001 EAE Sal. vs EAE PM: n.s.
4d	Two-way Anova	CTRL Saline = 8 CTRL PM = 8 EAE Saline = 7	Immunization Effect: P= 0,0979 Exposure Effect: P= 0,2523	Immunization: F (1, 26) = 2,947 Exposure: F (1, 26) = 1,371	Bonferroni's Multiple Comparisons Test	CTRL Sal. vs CTRL PM: n.s. CTRL Sal. vs EAE Sal.: n.s. CTRL PM vs EAE PM: P= 0,0174

		EAE PM = 7	Immunization x Exposure: P= 0,0069	Immunization x Exposure: F (1, 26) = 8,595		EAE Sal. vs EAE PM: n.s.
4f	Two-way Anova	CTRL Saline = 8 CTRL PM = 8 EAE Saline = 8 EAE PM = 7	Immunization Effect: P <0,0001 Exposure Effect: P= 0,4776 Immunization x Exposure: P= 0,9425	Immunization: F (1, 27) = 41,91 Exposure: F (1, 27) = 0,5187 Immunization x Exposure: F (1, 27) = 0,005305	Bonferroni's Multiple Comparisons Test	CTRL Sal. vs CTRL PM: n.s. CTRL Sal. vs EAE Sal.: P= 0,0005 CTRL PM vs EAE PM: P= 0,0006 EAE Sal. vs EAE PM: n.s.
4g	Two-way Anova	CTRL Saline = 8 CTRL PM = 8 EAE Saline = 8 EAE PM = 7	Immunization Effect: P= 0,0839 Exposure Effect: P= 0,0007 Immunization x Exposure: P= 0,0007	Immunization: F (1, 27) = 3,220 Exposure: F (1, 27) = 14,81 Immunization x Exposure: F (1, 27) = 14,51	Bonferroni's Multiple Comparisons Test	CTRL Sal. vs CTRL PM: n.s. CTRL Sal. vs EAE Sal.: n.s. CTRL PM vs EAE PM: P= 0,0035 EAE Sal. vs EAE PM: P <0,0001
4i	Two-way Anova	CTRL Saline = 8 CTRL PM = 8 EAE Saline = 8 EAE PM = 7	Immunization Effect: P= 0,0004 Exposure Effect: P= 0,2362 Immunization x Exposure: P= 0,9541	Immunization: F (1, 27) = 16,32 Exposure: F (1, 27) = 1,468 Immunization x Exposure: F (1, 27) = 0,003373	Bonferroni's Multiple Comparisons Test	CTRL Sal. vs CTRL PM: n.s. CTRL Sal. vs EAE Sal.: P= 0,0479 CTRL PM vs EAE PM: P= 0,0498 EAE Sal. vs EAE PM: n.s.
4j	Two-way Anova	CTRL Saline = 8 CTRL PM = 8 EAE Saline = 8	Immunization Effect: P=<0,0001 Exposure Effect: P= 0,0065	Immunization: F (1, 27) = 80,16 Exposure: F (1, 27) = 8,702 Immunization x Exposure: F	Bonferroni's Multiple Comparisons Test	CTRL Sal. vs CTRL PM: n.s. CTRL Sal. vs EAE Sal.: P <0,0001

		EAE PM = 7	Immunization x Exposure: P= 0,9541	(1, 27) = 0,003368		CTRL PM vs EAE PM: P <0,0001 EAE Sal. vs EAE PM: n.s.
4k	Two-way Anova	CTRL Saline = 8 CTRL PM = 8 EAE Saline = 8 EAE PM = 7	Immunization Effect: P= 0,4009 Exposure Effect: P= 0,0195 Immunization x Exposure: P= 0,0776	Immunization: F (1, 27) = 0,7285 Exposure: F (1, 27) = 6,164 Immunization x Exposure: F (1, 27) = 3,367	Bonferroni's Multiple Comparisons Test	CTRL Sal. vs CTRL PM: n.s. CTRL Sal. vs EAE Sal.: n.s. CTRL PM vs EAE PM: n.s. EAE Sal. vs EAE PM: P= 0,0343
4m	Two-way Anova	CTRL Saline = 8 CTRL PM = 8 EAE Saline = 8 EAE PM = 7	Immunization Effect: P= 0,0004 Exposure Effect: P= 0,8396 Immunization x Exposure: P= 0,3875	Immunization: F (1, 27) = 16,29 Exposure: F (1, 27) = 0,04179 Immunization x Exposure: F (1, 27) = 16,29	Bonferroni's Multiple Comparisons Test	CTRL Sal. vs CTRL PM: n.s. CTRL Sal. vs EAE Sal.: n.s. CTRL PM vs EAE PM: P= 0,0121 EAE Sal. vs EAE PM: n.s.
4n	Two-way Anova	CTRL Saline = 8 CTRL PM = 8 EAE Saline = 8 EAE PM = 7	Immunization Effect: P= 0,0322 Exposure Effect: P= 0,6813 Immunization x Exposure: P= 0,4743	Immunization: F (1, 27) = 5,099 Exposure: F (1, 27) = 0,1724 Immunization x Exposure: F (1, 27) = 0,5266	Bonferroni's Multiple Comparisons Test	CTRL Sal. vs CTRL PM: n.s. CTRL Sal. vs EAE Sal.: n.s. CTRL PM vs EAE PM: n.s. EAE Sal. vs EAE PM: n.s.
4p	Two-way Anova	CTRL Saline = 8 CTRL PM = 8 EAE Saline = 8 EAE PM = 7	Immunization Effect: P= 0,1779 Exposure Effect: P= 0,0062 Immunization x Exposure: P= 0,4262	Immunization: F (1, 27) = 1,913 Exposure: F (1, 27) = 8,809 Immunization x Exposure: F (1, 27) = 0,6526	Bonferroni's Multiple Comparisons Test	CTRL Sal. vs CTRL PM: n.s. CTRL Sal. vs EAE Sal.: n.s. CTRL PM vs EAE PM: n.s. EAE Sal. vs EAE PM: n.s.

4q	Two-way Anova	CTRL Saline = 8 CTRL PM = 8 EAE Saline = 8 EAE PM = 7	Immunization Effect: P= 0,0006 Exposure Effect: P= 0,0034 Immunization x Exposure: P= 0,4877	Immunization: F (1, 27) = 15,11 Exposure: F (1, 27) = 10,35 Immunization x Exposure: F (1, 27) = 0,4950	Bonferroni's Multiple Comparisons Test	CTRL Sal. vs CTRL PM: n.s. CTRL Sal. vs EAE Sal.: P= 0,0162 CTRL PM vs EAE PM: n.s. EAE Sal. vs EAE PM: n.s.
4s	Two-way Anova	CTRL Saline = 8 CTRL PM = 8 EAE Saline = 8 EAE PM = 7	Immunization Effect: P= <0,0001 Exposure Effect: P= 0,5425 Immunization x Exposure: P= 0,4251	Immunization: F (1, 27) = 145,8 Exposure: F (1, 27) = 0,3804 Immunization x Exposure: F (1, 27) = 0,6558	Bonferroni's Multiple Comparisons Test	CTRL Sal. vs CTRL PM: n.s. CTRL Sal. vs EAE Sal.: P <0,0001 CTRL PM vs EAE PM: P <0,0001 EAE Sal. vs EAE PM: n.s.
4t	Two-way Anova	CTRL Saline = 8 CTRL PM = 8 EAE Saline = 8 EAE PM = 7	Immunization Effect: P= <0,0001 Exposure Effect: P= 0,0047 Immunization x Exposure: P= 0,0391	Immunization: F (1, 27) = 161,2 Exposure: F (1, 27) = 9,471 Immunization x Exposure: F (1, 27) = 0,04920	Bonferroni's Multiple Comparisons Test	CTRL Sal. vs CTRL PM: n.s. CTRL Sal. vs EAE Sal.: P <0,0001 CTRL PM vs EAE PM: P <0,0001 EAE Sal. vs EAE PM: n.s.
5a	Two-way Anova	CTRL Saline = 5 CTRL PM = 4 EAE Saline = 3 EAE PM = 4	Immunization Effect: P= 0,0391 Exposure Effect: P= 0,4309 Immunization x Exposure: P= 0,0670	Immunization: F (1, 12) = 5,362 Exposure: F (1, 12) = 0,6645 Immunization x Exposure: F (1, 12) = 4,056	Bonferroni's Multiple Comparisons Test	CTRL Sal. vs CTRL PM: n.s. CTRL Sal. vs EAE Sal.: n.s. CTRL PM vs EAE PM: n.s EAE Sal. vs EAE PM: n.s
5b	(See Suppl. Figure 2 a-m)					

Suppl. 1a		CTRL Saline = 8 CTRL PM = 8 EAE Saline = 8 EAE PM = 7	Immunization Effect: P<0,0001 Exposure Effect: P= 0,0516 Immunization x Exposure: P= 0,3021	Immunization: F (1, 27) = 164,0 Exposure: F (1, 27) = 4,147 Immunization x Exposure: F (1, 27) = 1,107		CTRL Sal. vs CTRL PM: n.s. CTRL Sal. vs EAE Sal.: P<0,0001 CTRL PM vs EAE PM: P<0,0001 EAE Sal. vs EAE PM: n.s
Suppl. 1b		CTRL Saline = 8 CTRL PM = 8 EAE Saline = 8 EAE PM = 7	Immunization Effect: P=0,0040 Exposure Effect: P=0,5101 Immunization x Exposure: P=0,5164	Immunization: F (1, 27) = 9,887 Exposure: F (1, 27) = 0,4456 Immunization x Exposure: F (1, 27) = 0,4324		CTRL Sal. vs CTRL PM: n.s. CTRL Sal. vs EAE Sal.: n.s. CTRL PM vs EAE PM: n.s EAE Sal. vs EAE PM: n.s
Suppl. 2a	Two-way Anova	n=5	Immunization Effect: P= 0,0010 Exposure Effect: P= 0,5168 Immunization x Exposure: P=0,7645	Immunization: F (1, 16) = 16,04 Exposure: F (1, 16) = 0,4395 Immunization x Exposure: F (1, 16) = 0,09285	Bonferroni's Multiple Comparisons Test	CTRL Sal. vs CTRL PM: n.s. CTRL Sal. vs EAE Sal.: P=0,0461 CTRL PM vs EAE PM: n.s. EAE Sal. vs EAE PM: n.s.
Suppl. 2b	Two-way Anova	n=5	Immunization Effect: P= 0,0074 Exposure Effect: P= 0,4974 Immunization x Exposure: P= 0,1432	Immunization: F (1, 16) = 9,381 Exposure: F (1, 16) = 0,4821 Immunization x Exposure: F (1, 16) = 2,371	Bonferroni's Multiple Comparisons Test	CTRL Sal. vs CTRL PM: n.s. CTRL Sal. vs EAE Sal.: P=0,0298 CTRL PM vs EAE PM: n.s. EAE Sal. vs EAE PM: n.s.
Suppl. 2c	Two-way Anova	n=5	Immunization Effect: P= 0,7646	Immunization: F (1, 16) = 0,09278	Bonferroni's Multiple Comparisons Test	CTRL Sal. vs CTRL PM: n.s. CTRL Sal. vs EAE Sal.: n.s.

			Exposure Effect: P= 0,2233 Immunization x Exposure: P= 0,4585	Exposure: F (1, 16) = 1,605 Immunization x Exposure: F (1, 16) = 0,5771		CTRL PM vs EAE PM: n.s. EAE Sal. vs EAE PM: n.s.
Suppl. 2d	Two-way Anova	n=5	Immunization Effect: P= 0,2720 Exposure Effect: P= 0,3593 Immunization x Exposure: P= 0,8272	Immunization: F (1, 16) = 1,295 Exposure: F (1, 16) = 0,8907 Immunization x Exposure: F (1, 16) = 0,04924	Bonferroni's Multiple Comparisons Test	CTRL Sal. vs CTRL PM: n.s. CTRL Sal. vs EAE Sal.: n.s. CTRL PM vs EAE PM: n.s. EAE Sal. vs EAE PM: n.s.
Suppl. 2e	Two-way Anova	CTRL Saline = 5 CTRL PM = 5 EAE Saline = 4 EAE PM = 5	Immunization Effect: P= 0,7755 Exposure Effect: P= 0,3034 Immunization x Exposure: P= 0,5833	Immunization: F (1, 15) = 0,08432 Exposure: F (1, 15) = 1,136 Immunization x Exposure: F (1, 15) = 0,3144	Bonferroni's Multiple Comparisons Test	CTRL Sal. vs CTRL PM: n.s. CTRL Sal. vs EAE Sal.: n.s. CTRL PM vs EAE PM: n.s. EAE Sal. vs EAE PM: n.s.
Suppl. 2f	Two-way Anova	n=5	Immunization Effect: P= 0,1972 Exposure Effect: P= 0,8096 Immunization x Exposure: P= 0,3504	Immunization: F (1, 16) = 1,810 Exposure: F (1, 16) = 0,06002 Immunization x Exposure: F (1, 16) = 0,9254	Bonferroni's Multiple Comparisons Test	CTRL Sal. vs CTRL PM: n.s. CTRL Sal. vs EAE Sal.: n.s. CTRL PM vs EAE PM: n.s. EAE Sal. vs EAE PM: n.s.
Suppl. 2g	Two-way Anova	n=5	Immunization Effect: P= 0,0266 Exposure Effect: P= 0,9328 Immunization x Exposure: P= 0,5148	Immunization: F (1, 16) = 5,960 Exposure: F (1, 16) = 0,007331 Immunization x Exposure: F (1, 16) = 0,4438	Bonferroni's Multiple Comparisons Test	CTRL Sal. vs CTRL PM: n.s. CTRL Sal. vs EAE Sal.: n.s. CTRL PM vs EAE PM: n.s. EAE Sal. vs EAE PM: n.s.

Suppl. 2h	Two-way Anova	CTRL Saline = 5 CTRL PM = 5 EAE Saline = 4 EAE PM = 5	Immunization Effect: P= 0,7284 Exposure Effect: P= 0,5038 Immunization x Exposure: P= 0,0925	Immunization: F (1, 14) = 0,1256 Exposure: F (1, 14) = 0,4708 Immunization x Exposure: F (1, 14) = 3,260	Bonferroni's Multiple Comparisons Test	CTRL Sal. vs CTRL PM: n.s. CTRL Sal. vs EAE Sal.: n.s. CTRL PM vs EAE PM: n.s. EAE Sal. vs EAE PM: n.s.
Suppl. 2i	Two-way Anova	CTRL Saline = 5 CTRL PM = 5 EAE Saline = 4 EAE PM = 5	Immunization Effect: P= 0,5779 Exposure Effect: P= 0,4003 Immunization x Exposure: P= 0,9957	Immunization: F (1, 15) = 0,3236 Exposure: F (1, 15) = 0,7495 Immunization x Exposure: F (1, 15) = 2,972e-005	Bonferroni's Multiple Comparisons Test	CTRL Sal. vs CTRL PM: n.s. CTRL Sal. vs EAE Sal.: n.s. CTRL PM vs EAE PM: n.s. EAE Sal. vs EAE PM: n.s.
Suppl. 2j	Two-way Anova	CTRL Saline = 5 CTRL PM = 5 EAE Saline = 4 EAE PM = 5	Immunization Effect: P= 0,0050 Exposure Effect: P= 0,4871 Immunization x Exposure: P= 0,7321	Immunization: F (1, 15) = 10,81 Exposure: F (1, 15) = 0,5077 Immunization x Exposure: F (1, 15) = 0,1217	Bonferroni's Multiple Comparisons Test	CTRL Sal. vs CTRL PM: n.s. CTRL Sal. vs EAE Sal.: n.s. CTRL PM vs EAE PM: n.s. EAE Sal. vs EAE PM: n.s.
Suppl. 2k	Two-way Anova	n=5	Immunization Effect: P= 0,0014 Exposure Effect: P= 0,8703 Immunization x Exposure: P= 0,6544	Immunization: F (1, 16) = 14,74 Exposure: F (1, 16) = 0,02752 Immunization x Exposure: F (1, 16) = 0,2081	Bonferroni's Multiple Comparisons Test	CTRL Sal. vs CTRL PM: n.s. CTRL Sal. vs EAE Sal.: P=0,0471 CTRL PM vs EAE PM: n.s. EAE Sal. vs EAE PM: n.s.
Suppl. 2l	Two-way Anova	n=5	Immunization Effect: P= 0,0819 Exposure Effect: P= 0,2364	Immunization: F (1, 16) = 3,446 Exposure: F (1, 16) = 1,513	Bonferroni's Multiple Comparisons Test	CTRL Sal. vs CTRL PM: n.s. CTRL Sal. vs EAE Sal.: n.s.

			Immunization x Exposure: P= 0,6178	Immunization x Exposure: F (1, 16) = 0,2589		CTRL PM vs EAE PM: n.s. EAE Sal. vs EAE PM: n.s.
Suppl. 2m	Two-way Anova	n=5	Immunization Effect: P= 0,0280 Exposure Effect: P= 0,9420 Immunization x Exposure: P= 0,8449	Immunization: F (1, 16) = 5,842 Exposure: F (1, 16) = 0,005471 Immunization x Exposure: F (1, 16) = 0,03952	Bonferroni's Multiple Comparisons Test	CTRL Sal. vs CTRL PM: n.s. CTRL Sal. vs EAE Sal.: n.s. CTRL PM vs EAE PM: n.s. EAE Sal. vs EAE PM: n.s.

Supplementary Table 2 - qRT-PCR Assays

Gene	Abbreviation	Biological Role	Primers/Probe
Dopamine Receptor D1	Drd1	dopamine receptor	Primer FW: CATCAACAACAACGGGGCTG Primer RV: AGTCCTTGGAGATGGAGCCT UPL Probe #83
Dopamine Receptor D2	Drd2	dopamine receptor	Primer FW: ATCATTGCCAACCCTGCCTT Primer RV: GTGACGATGAAGGGCACGTA UPL Probe #25
Solute Carrier family 6 member 3	Slc6a3 (Dat)	dopamine re-uptake	Primer FW: CTACATGGAGCTGGCTCTCG Primer RV: CAGGACAGGGCAGATCTTCC UPL Probe #17
Tyrosine Hydroxylase	Th	rate limiting enzyme in dopamine biosynthesis	Primer FW: GGAACGGTACTGTGGCTACC Primer RV: GCCAGTCCGTTCCTTCAAGA UPL Probe #78
Monoamine Oxidase A	MaoA	dopamine catabolism	Primer FW: GTGATTCGGCAGCCAGTAGG Primer RV: GCACCTTCCATGTAGCCACT UPL Probe #98
Monoamine Oxidase B	MaoB	dopamine catabolism	Primer FW: CTTTGGATGTCCCTGCACGA Primer RV: GCTTTAGCAGGCCTGGTACA UPL Probe #80
Cathecol-O-methyltransferase	Comt	dopamine catabolism	Primer FW: GAAGTCCTGACCACTCAGCC Primer RV: GGGGTCAGAGTGAGTGTGTG UPL Probe #24
Dopamine Beta Hydroxylase	Dbh	conversion of dopamine to norepinephrine	Primer FW: CGCCCCTATCTCCATGCATT Primer RV: AGGCTGCAGATTCCACTCAC UPL Probe #56
Solute Carrier family 18 member 2	Slc18a2 (Vmat2)	dopamine vesicular transporter (dopamine release	Primer FW: CCCCTTTGGAAGTGTGCTCT Primer RV: ATCCAAGAGCACCAAGGCAG

		in the synaptic cleft)	UPL Probe #17
Ras-like without CAAX 2	Rit2	involved in DAT internalization	Primer FW: GAGGCTGCCAAGTTCAAGGA Primer RV: TACCCACTAGCACAAGGGGA UPL Probe #85
VPS35 Retromer Complex Component	Vps35	involved in DRD1 trafficking and dopamine mediated signaling	Primer FW: ACATTTTGGGGCTGGTGGAA Primer RV: AGCCAACTGGTAAGCTGCAA UPL Probe #87
Leucine-rich Repeat Kinase 2	Lrrk2	limitation of DRD1 signaling	Primer FW: GTCCAGGAAGGCAAGCAGAT Primer RV: CGGTCCGAGTAGGTGAACAC UPL Probe #17
Parkin RBR E3 Ubiquitin Protein Ligase	Prkn	involved in DAT ubiquitination and degradation	Primer FW: AGGAAAGTCACCTGCGAAGG Primer RV: CTTCCTTACAGTCCCGGCAG UPL Probe #26